

Green Chemistry

Accepted Manuscript



This is an *Accepted Manuscript*, which has been through the Royal Society of Chemistry peer review process and has been accepted for publication.

Accepted Manuscripts are published online shortly after acceptance, before technical editing, formatting and proof reading. Using this free service, authors can make their results available to the community, in citable form, before we publish the edited article. We will replace this *Accepted Manuscript* with the edited and formatted *Advance Article* as soon as it is available.

You can find more information about *Accepted Manuscripts* in the [Information for Authors](#).

Please note that technical editing may introduce minor changes to the text and/or graphics, which may alter content. The journal's standard [Terms & Conditions](#) and the [Ethical guidelines](#) still apply. In no event shall the Royal Society of Chemistry be held responsible for any errors or omissions in this *Accepted Manuscript* or any consequences arising from the use of any information it contains.



www.rsc.org/greenchem

A nickel doped perovskite catalyst for reforming methane rich biogas with minimal carbon deposition†

Samuel E. Evans*, John Z. Staniforth, Richard J. Darton, R. Mark Ormerod*

Catalysis and Sustainable Materials Group, Lennard-Jones Laboratories, School of Physical and Geographical Sciences, Keele University, Staffordshire, ST5 5BG, United Kingdom

† A patent application based on the results presented here has been filed through Keele University. UK Patent number GB1321230.3.

Abstract

A novel nickel-doped strontium zirconate perovskite catalyst for biogas reforming has been synthesised using a green, low temperature hydrothermal synthesis. The catalyst has been shown to be very efficient towards the conversion of methane-rich biogas at relatively low temperatures with high selectivity towards synthesis gas formation and extremely good resistance to carbon deposition in carbon-rich reaction mixtures. The catalyst displays very low carbon deposition which does not increase over time, and as a result shows excellent stability. The use of a catalyst produced by a low temperature hydrothermal route provides a potentially very attractive and sustainable source of useful chemicals from biogas that otherwise might be vented wastefully and detrimentally into the atmosphere.

1. Introduction

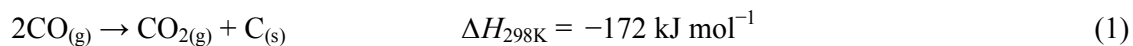
The increasing dependence on limited oil and gas reserves is an increasingly critical global scientific, technical and political challenge. This has intensified the requirement for alternative sources of energy production and storage and production of useful chemicals globally. Currently steam reforming is the most commonly used method for the production of synthesis gas from methane or natural gas. However this gives a high H₂: CO ratio that,

while useful for hydrogen production, is stoichiometrically unfavourable for the Fischer-Tropsch process and oxygenate synthesis.

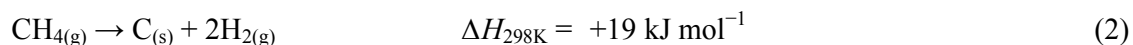
Carbon dioxide ('dry') reforming of methane is a reaction of particular interest as it utilises two greenhouse gases (CH_4 and CO_2) into synthesis gas (H_2 and CO)¹⁻⁴ which can then be used as a feedstock for production of higher hydrocarbons via the Fischer-Tropsch process or for the production of oxygenates^{5,6}. Biogas is produced via the anaerobic digestion of plant matter, animal and human waste, and other organic material^{7,8}. The composition of biogas is highly variable, but typically consists of an approximately 2:1 ratio of methane to carbon dioxide, as well as containing relatively high levels of sulphur in the form of hydrogen sulphide, and other minor impurities, such as halides, depending on the source^{9,10}. The high carbon dioxide content makes biogas a difficult fuel to work with in traditional ways as combustion is problematic when the concentration of CO_2 exceeds 50%¹¹. The presence of both methane and carbon dioxide in biogas in significant quantities means that dry reforming of methane is a particularly relevant reaction in relation to catalytic conversion of biogas into useful products.

Currently oxide supported nickel catalysts are commonly used for the production of synthesis gas from methane, however supported nickel catalysts are susceptible to carbonaceous build-up, particularly in the absence of a significant excess of oxidant¹²⁻¹⁴. Carbon deposits have several detrimental effects on supported nickel catalysts. Carbon can react directly with nickel to form nickel carbide, reducing the number of reactive nickel sites^{15,16} or deposit within the nickel porous structure, expanding and destroying the microstructure¹⁷. Furthermore carbon can restrict the flow of reactant gases to the point that gas flow ceases entirely. One of the major issues with carbon deposition is that it occurs over a range of

temperatures. At low temperatures carbon can be deposited due to the disproportionation of carbon monoxide, the Boudouard reaction¹⁸ (eqn. 1):



At higher temperatures thermal decomposition of methane (eqn. 2) becomes increasingly favourable



This means that there are no reaction temperatures which give a thermodynamically carbon free system whilst maintaining the required reaction products. As a result of this the development of an alternative catalytic material to give the desired product selectivity without deleterious carbon build-up is highly desirable

Much research has focused on the use of supported nickel catalysts for the production of synthesis gas from methane due to its relatively low cost compared to precious metal catalysts such as rhodium and platinum¹⁹⁻²¹. However, supported nickel catalysts are particularly susceptible to carbon deposition which leads to catalyst deactivation^{22,23}, through methane decomposition in particular (eqn. 2) and the Boudouard reaction (eqn. 1). Carbon deposition is a particular problem with nickel catalysts for reforming methane when the oxidant is carbon dioxide^{24,25}; with steam reforming a significant excess of steam is added to avoid carbon deposition, typically a steam:methane ratio of around 2.5 is used in commercial steam reforming plants^{12,26,27}.

Research into reforming methane using carbon dioxide for generation of electricity via direct internal reforming solid oxide fuel cells (DIR-SOFC) is work of increasing scientific interest^{11,28-31}. However, the current anode technology for utilising this fuel source in SOFCs; nickel supported on yttria stabilised zirconia (Ni/YSZ), has lifetime issues that prevents this technology from being commercially viable to date^{32,33}.

Ni/YSZ can suffer from deposits of solid carbon via several different reaction pathways including thermal decomposition (2) and the Boudouard reaction (1)¹⁸, leading to failure of the cell. This occurs due to the disruption of micro-pore systems at the anode³⁴, and also restriction in the fuel supply, resulting in the cell becoming starved of fuel.

A further issue that can be more detrimental than carbon deposition is sulphur poisoning. This is caused by sulphur containing compounds in the biogas that are generated during the digestion process. Sulphur concentrations as low as a few parts per billion can cause loss of catalytic activity at the anode³⁵. This can be attributed to formation of stable nickel-sulphur species that lower and eventually eliminate the number of active sites available for the reforming reaction. The resistance of this material to poisoning caused by sulphur containing compounds will be discussed in a future paper.

Perovskite materials have been shown to be catalytically active for methane conversion and show a lesser propensity to form carbon at lower cost than noble metals³. Early work by Libby *et al* showed that $\text{Sr}_{0.2}\text{La}_{0.8}\text{CoO}_3$ rivalled platinum for reactions at a far lower cost and showed potential as a catalyst for use in vehicle exhausts³⁶. To date several perovskites have been reported as potential alternative catalyst materials to nickel for reforming methane under partial oxidation conditions^{37,38}, steam reforming conditions²⁶ and dry reforming³⁹.

However, these all show low activity and/or selectivity towards synthesis gas, with the more active materials favouring production of total oxidation products.

The perovskite structure has been shown to be extremely versatile, with minor changes to the composition altering the catalytic activity significantly. Sfeir *et al*⁴⁰ investigated substituted lanthanum chromites for the oxidation of methane reaction. These perovskite type catalysts had relatively low surface areas; between 1-3 m² g⁻¹ and despite being active for the partial oxidation of methane, methane conversion was seen to be significantly lower than the maximum achievable conversion.

Zhan *et al* reported a La₄Sr₈Ti₁₂O_{38.8} perovskite catalyst synthesised using a sol-gel route³⁸. The catalyst had a BET surface area of 8.2 m² g⁻¹ and a cubic perovskite type structure. The catalyst was tested for partial oxidation at 950 °C and compared to a supported nickel catalyst. It was found that under the tested conditions the supported nickel catalyst gave 84.1% methane conversion with almost total selectivity towards syngas production. The synthesised perovskite had a substantially lower conversion of methane of 30.1% despite the elevated reaction temperatures. The perovskite catalyst, although still quite selective for syngas production, as well as being less active, was also less selective for syngas formation, with selectivities of 87.8% and 88.0% for hydrogen and carbon monoxide production, respectively. The reduced selectivity was due to carbon dioxide production highlighting the propensity for perovskites to catalyse the formation of total oxidation products.

Standard preparation methods for producing perovskites involve heating together the oxides or carbonates of the required product ions at temperatures in excess of 1000 °C⁴¹. However, alternative methods have been shown to be more controllable, greener and can yield purer

products^{42,43}. Hydrothermal synthesis is a route that results in very small particle sizes, and as a result a high surface area product and can also yield products that cannot be synthesised by other methods^{44,45}. It has been shown in previous research that perovskites with the smallest particle size have the greatest catalytic activity towards the oxidation of methane⁴⁶. Hydrothermal synthesis utilises a sealed vessel such as an autoclave to bring solvents to higher temperatures than their respective boiling points by increasing the autogenous pressure⁴⁷. Reactions performed under the outlined conditions benefit from the increased solubility of the precursor materials, lowered cost due to the comparatively mild temperatures, and also the formation of crystalline products unlike sol-gel methods for example⁴⁸.

We recently reported a novel hydrothermally synthesised Ni doped SrZrO₃ perovskite and some initial catalytic results for methane reforming reactions^{49,50}. In this paper we describe dry reforming of methane over hydrothermally synthesised Ni doped SrZrO₃ perovskite under methane-rich conditions to mimic biogas. Using heavily methane rich simulated biogas maximises the potential for carbon formation. The carbon deposited on the catalyst surface during reaction is quantified using post-reaction temperature programmed oxidation (TPO) by integrating the produced carbon monoxide and carbon dioxide peaks.

2. Experimental

Preparation of Catalysts

The 4 mol% Ni doped SrZrO₃ was prepared using a hydrothermal route to give a homogenous, high surface area product. Molar ratios of 1 ZrOCl₂·8H₂O (Alfa Aesar, 98%): 0.8 Sr(NO₃)₂ (Alfa Aesar, 99%): 0.2 Ni(NO₃)₂·6H₂O (Aldrich, 99%): 8 NaOH (Aldrich,

>97%) and ultra-pure water were all combined within a 23 ml Teflon lined stainless steel autoclave to produce the required stoichiometry. This was stirred until a homogeneous gel formed. The Teflon liner was then sealed inside the autoclave and placed within a forced air oven set to 180 °C for 72 hours. The autoclave was then removed and cooled to room temperature. The product was recovered by several cycles of centrifuging at 5000 rpm for 15 minutes and washing with distilled water. The sample was placed in an oven set to 60 °C for 24 hours and then ground to form a fine powder.

Nickel supported on yttria stabilised zirconia (Ni/YSZ) was prepared by the standard physical mixing method that gave a 90:10 nickel to YSZ ratio that has been previously used as the outer layer of a dual layer anode configuration of a SOFC⁵¹. This material also represents a good catalyst for the dry reforming of methane reaction. NiO (Alfa Aesar, 99%), YSZ (TOSOH, 11 mol% Y), trichloroethene (Aldrich, 99%), methanol (Aldrich, 99%) and glyceroltrioleate (Aldrich, 99%) in appropriate amounts were milled for 4 hours in a ball mill to form a homogenous slurry. 0.15 g of polyvinyl butyral (BDH Chemicals Ltd) was then added as a binding agent and the mix further milled for 10 minutes. This was then transferred into ceramic boats and sintered on a temperature programme of 1 °C min⁻¹ up to 500 °C, then 5 °C min⁻¹ up to 1200 °C and held for 1 hour. The resulting material was ground to form a fine powder and placed in an oven set to 60 °C overnight.

Characterisation of Catalysts

The structures of the catalyst materials were analysed using powder X-ray diffraction (XRD) and BET analysis. X-ray diffraction was carried out using a Bruker D8 Advance powder X-ray diffractometer using CuK α radiation. BET analysis was collected using a Quantachrome Autosorb-1-C instrument using N₂ gas.

3. Catalytic Testing

Test Rig

Catalytic testing was undertaken using custom built 'rigs'. All gases used were BOC high purity gases and contained within pressurised cylinders with a gas supply pressure of 1 bar. Each rig has inlet feeds for gases that are channelled through stainless steel piping into pre-calibrated mass flow controllers (MFCs). The gases are then passed to a manifold, where they are mixed, and each gas can be turned on or off independently. The gas mix was then sent through a furnace in which the catalyst is contained within a quartz reactor tube. The product gases pass into a quadrupole mass spectrometer (QMS) where up to 12 separate mass fragments can be analysed in essentially real time. The furnace temperature was maintained and monitored by a Eurotherm 310 system with a K-type thermocouple which also has the capability to perform temperature controlled reactions either isothermally or by linear temperature programmed reaction from 5 °C min⁻¹ up to 20 °C min⁻¹.

Temperature Programmed Reduction

To activate the catalyst material prior to reforming experiments the catalyst was first reduced. 20.0 ± 0.5 mg of the catalyst material was weighed out on a four decimal place balance and placed into a quartz reactor tube between two quartz wool plugs. The reactor tube was then fixed into the rig system using Cajon fittings. A 20% concentration of hydrogen in a helium carrier was passed through the tube at 20 ml min⁻¹ and reduction was carried out using a programme of 10 °C min⁻¹ up to a temperature of 850 °C. The furnace was cooled to room temperature with the hydrogen mixture still passing through the reactor tube. Upon reaching room temperature bypass helium was diverted over the catalyst.

Simulated Biogas Reformation

The reactant gas composition was set up with the reactant feed bypassing the furnace, with helium passing through the reactor to maintain an inert atmosphere for the reduced catalyst. The mass flow controllers were adjusted to give a flow of 1 ml min⁻¹ of methane, 0.5 ml min⁻¹ of carbon dioxide and 18.5 ml min⁻¹ of helium. In the case of isothermal reactions the furnace was adjusted to the required temperature before reactant gases were diverted to the furnace. For temperature programmed reactions the furnace was ramped at 10 °C min⁻¹ up to 1000 °C from room temperature with reactant gases passing over the catalyst. All reactions were followed by QMS with a scan rate of a complete cycle every 12 seconds.

Temperature Programmed Oxidation

After each reaction was performed, the furnace was allowed to cool to room temperature with an inert flow of helium passing over the catalyst. After cooling a 20% concentration of oxygen in a helium carrier was passed over the catalyst at 20 ml min⁻¹ with the furnace set to a temperature programme of 10 °C min⁻¹ up to 900 °C. The resulting profile for carbon dioxide and carbon monoxide can be quantified using a predetermined calibration to give a mass for solid carbon deposited and the peak production profiles can be used to make inferences to the types of carbon present.

4. Results and Discussion

Characterisation

XRD and BET analysis of the 4 mol% Ni doped SrZrO₃ catalyst was undertaken prior to reduction of the material. All the diffraction peaks in figure 1 can be assigned to 4 mol% Ni doped SrZrO₃ with no discernible impurity peaks identifiable and this remained the case after

being washed with 1M nitric acid. This includes the lack of precursor peaks or possible by-products.

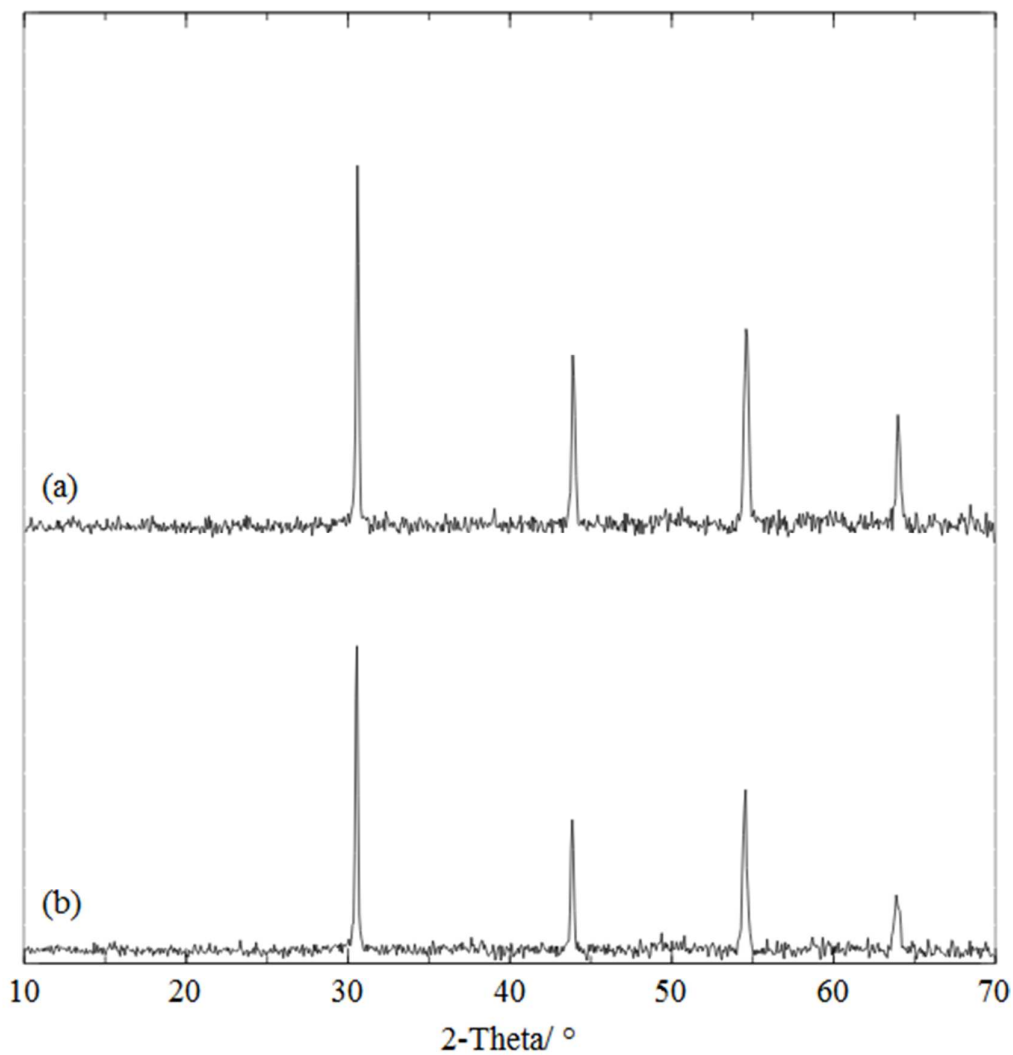


Figure 1 XRD pattern of (a) 4 mol% Ni doped SrZrO_3 (b) the same sample after washing with 1 M nitric acid for 30 minutes.

For heterogeneous catalysis the surface area of the catalyst material is a crucial factor in the complex array of parameters that determine the overall activity towards a specific reaction.

BET of the perovskite material gave an average surface area of ca. $38 \text{ m}^2 \text{ g}^{-1}$ and of ca. $1 \text{ m}^2 \text{ g}^{-1}$ for the Ni/YSZ material used.

X-Ray elemental analysis (EDAX) was performed (Hitachi TM3000 with a Bruker EDX analysis system) and confirms that the stoichiometry of the final product reflects the synthesis conditions, namely $\text{Ni}_{0.2}\text{Sr}_{0.8}\text{ZrO}_3$, which taken with the XRD pattern showing the formation of a crystalline single phase perovskite material with the absence of any discernible impurity peaks, implies that the nickel is located at the A-site of the perovskite structure as predicted by Beale *et al*⁵² for a hydrothermally synthesised nickel-doped strontium titanate material. There was no change in the stoichiometry as determined by EDAX analysis following washing with 1M nitric acid.

Initial analysis of the powder XRD pattern (Figure 2a) shows the material to be orthorhombic (Pbnm) with unit cell parameters of $a = 5.7948 \text{ \AA}$, $b = 5.8014 \text{ \AA}$ and $c = 8.1985 \text{ \AA}$, and with no presence of NiO or any other crystalline impurity phases⁴⁹. Although a slight change in some peak intensities is seen between the Ni doped and the un-doped SrZrO_3 materials (Figure 2), this is believed to be mainly due to preferred orientation and further work to elucidate the structure using neutron diffraction and EXAFS is currently underway.

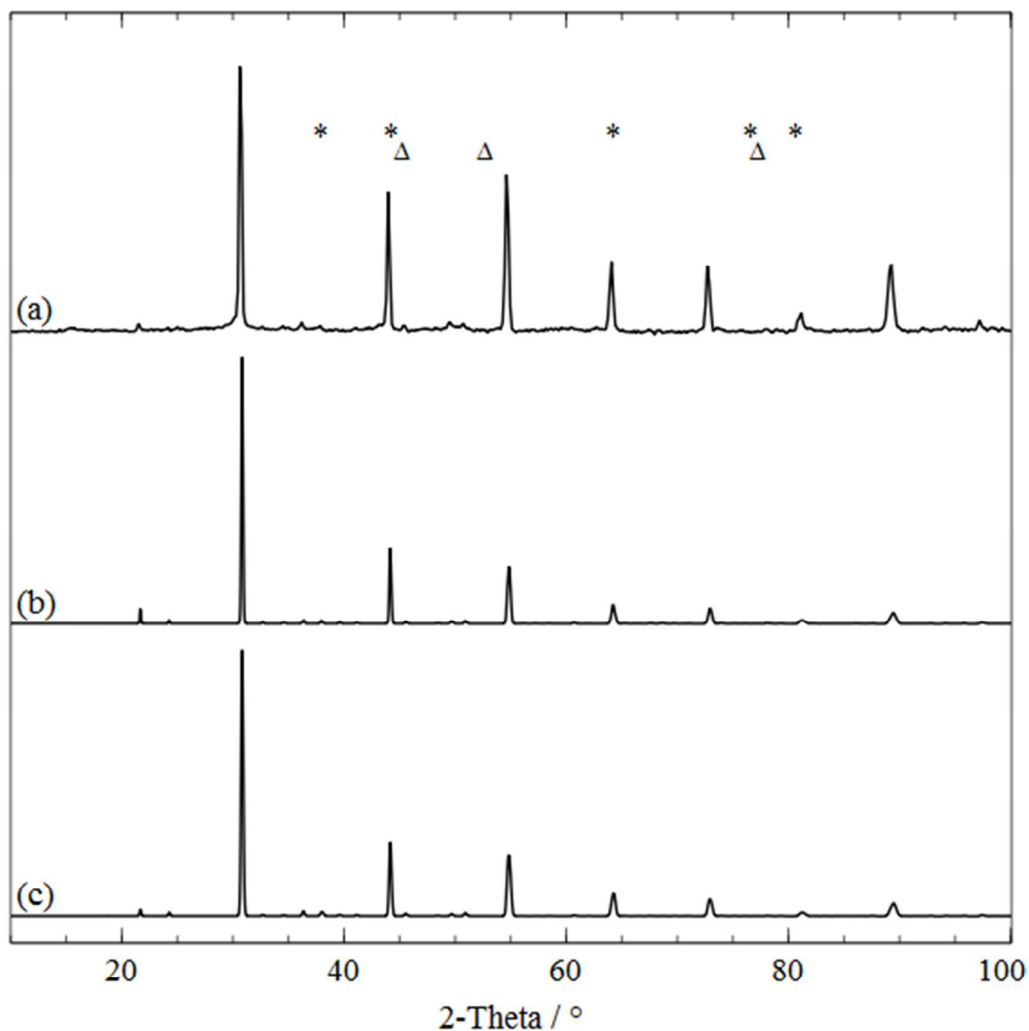


Figure 2 XRD pattern of (a) 4 mol% Ni doped SrZrO₃ (b) Simulated 4 mol% Ni doped SrZrO₃ (c) Simulated SrZrO₃; (*) denotes NiO peak positions; (Δ) denotes Ni peak positions

Catalysis

Temperature programmed reformation of simulated biogas (fig. 3) was performed on a reduced sample, with a 2:1 configuration of methane to carbon dioxide. No reaction was observed until 420 °C at which point dry reforming began. Methane and carbon dioxide levels fall together with complete consumption of carbon dioxide occurring by 800 °C. After 850 °C the H₂:CO ratio shifts to slightly higher than 1 suggesting that some thermal decomposition of methane occurs at the highest operating temperatures.

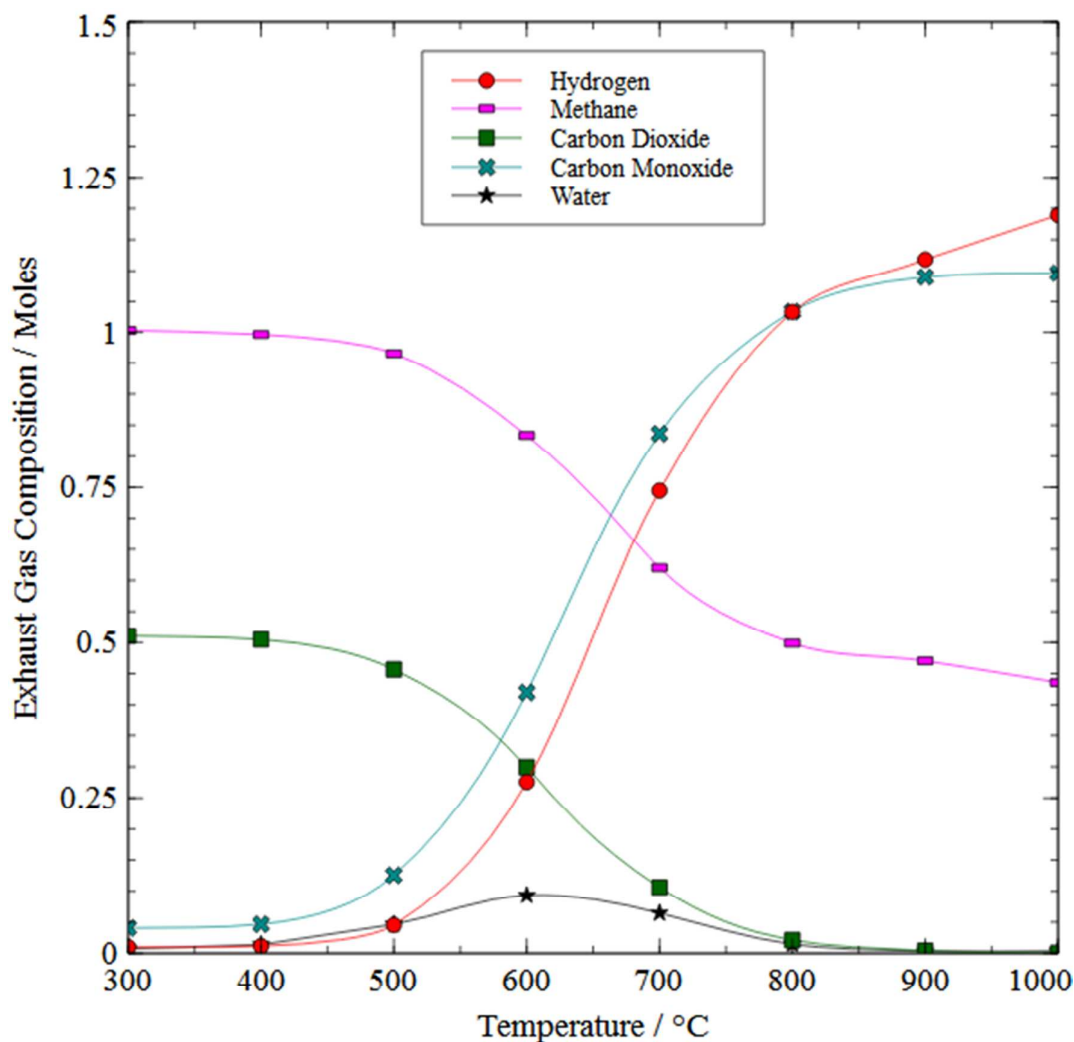


Figure 3 Temperature programmed biogas reformation over 4 mol% Ni doped SrZrO₃

Isothermal reactions at 700 °C, 800 °C and 900 °C were selected based on information from the temperature programmed reaction as suitable temperatures for complete, or near to complete carbon dioxide consumption. Identical reactions were also performed over Ni/YSZ for comparison purposes.

Figure 4 shows that almost complete reaction between methane and carbon dioxide was achieved at 700 °C, which is in agreement with thermodynamic predictions⁵³. Some carbon

dioxide however, was not utilised and this was reflected in the consumption of methane. The start-up time associated with the reaction is far shorter than has been reported for similar perovskite based catalysts for dry reforming⁵⁴, starting immediately with no apparent lag, and equilibrating in just a few hours. The reaction is also very selective towards the formation of synthesis gas with very little evidence of any side reactions occurring. Particularly there is no evidence of the occurrence of the Boudouard reaction, which is both thermodynamically and kinetically favoured over nickel based catalysts at this temperature due to the exothermic nature of the reaction and high concentration of carbon monoxide present³⁴.

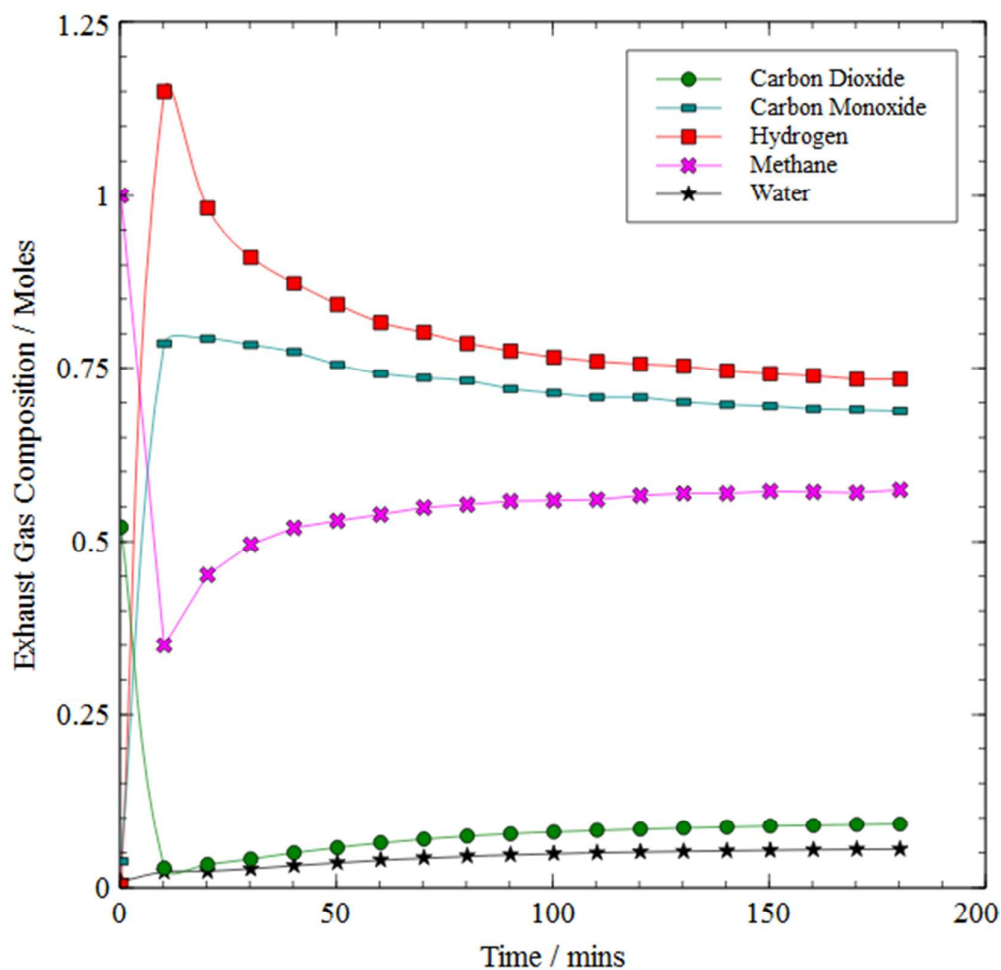


Figure 4: Biogas reformation at 700 °C for 3 hours over 4 mol% Ni doped SrZrO₃

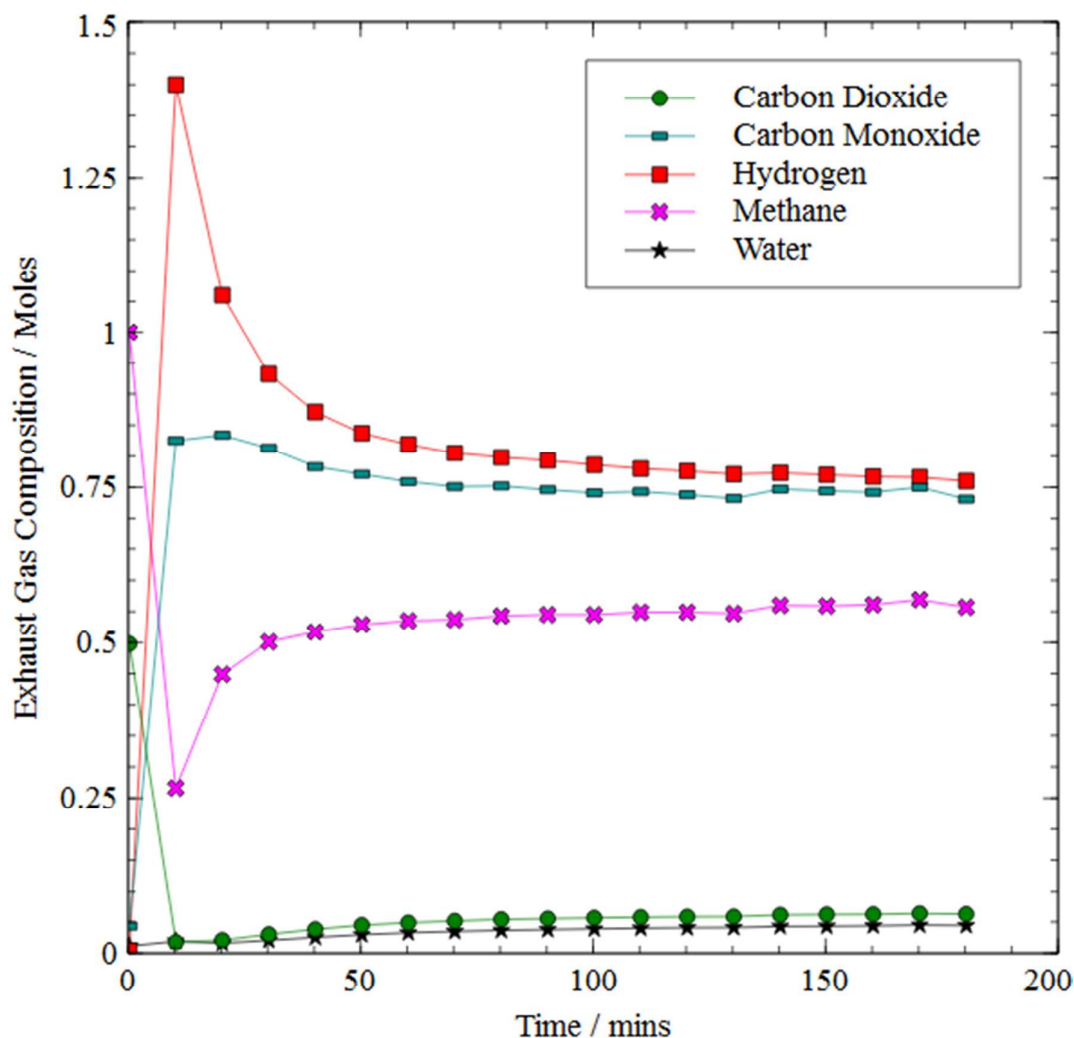


Figure 5: Biogas reformation at 800 °C for 3 hours over 4 mol% Ni doped SrZrO₃

It is predicted that by increasing the temperature to 800 °C the pyrolysis of methane would become the primary carbon forming reaction as the Boudouard reaction becomes more thermodynamically unfavourable. This would occur due to the decomposition of a portion of the excess methane resulting in the formation of carbon and hydrogen. For Ni/YSZ this is the case as can be seen in Table 1 with a methane conversion over 50%. For 4 mol% Ni doped SrZrO₃ the consumption of methane remains below 50% and this is confirmed by an almost 1:1 ratio of H₂: CO.

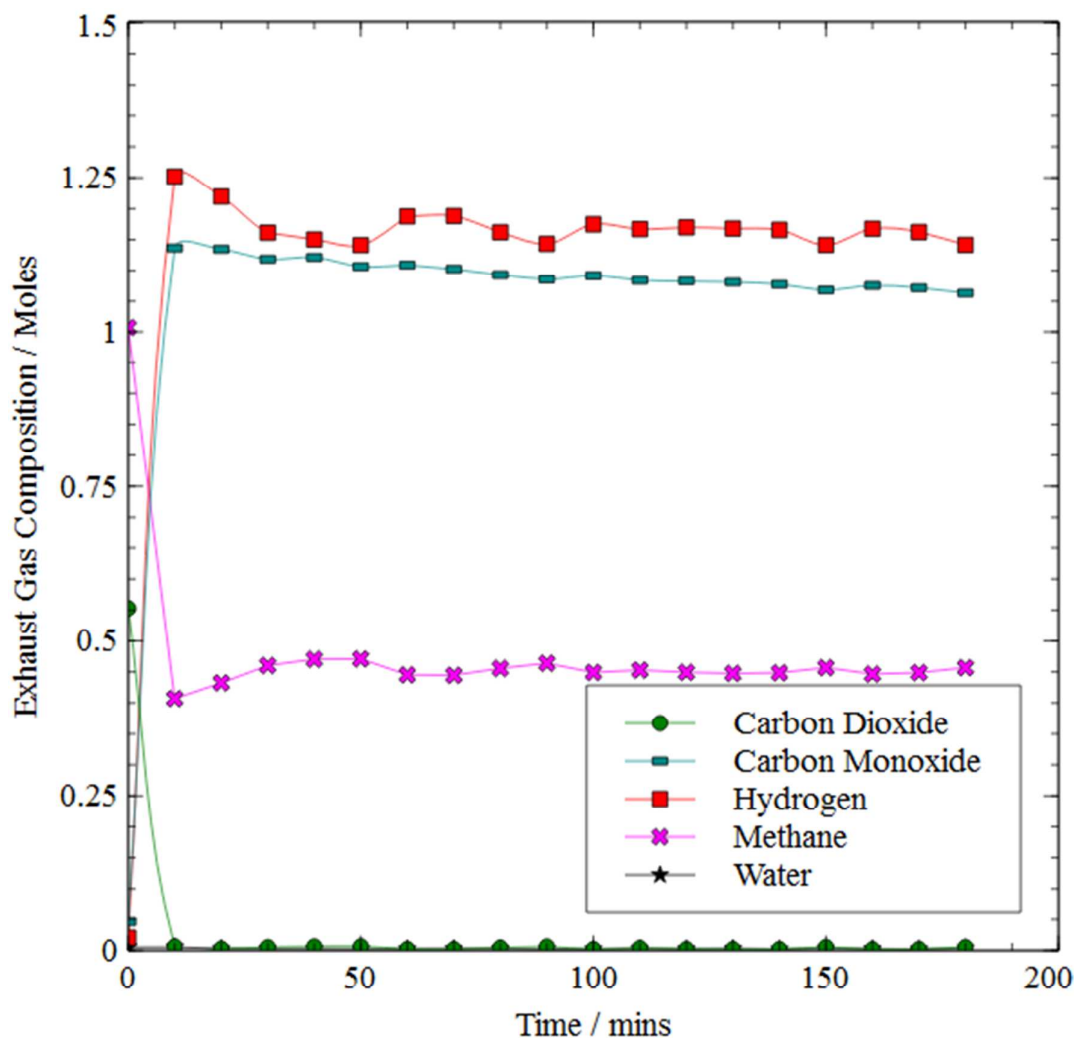


Figure 6: Biogas reformation at 900 °C for 3 hours over 4 mol% Ni doped SrZrO₃

At 900 °C methane decomposition is predicted to become quite prevalent, and it can be seen (fig. 6) that methane consumption is higher than predicted; this is reflected in the complete carbon dioxide consumption for the duration of the reaction. This methane pyrolysis leads to the highest H₂: CO ratio of the reactions performed. At 900 °C the stabilisation of the reaction happened faster than at 800 °C or 700 °C, with stability observed after 30 minutes. Although the methane pyrolysis is present in this reaction, the extent of this is lower than for Ni/YSZ as can be seen in Table 1.

Table 1 Comparison of methane and carbon dioxide conversion for 4 mol% Ni doped SrZrO₃ and Ni/YSZ after 3 hours on stream

Reforming Temperature (°C)	%Methane Conversion		%Carbon Dioxide Conversion	
	Ni/YSZ	4 mol% Ni doped SrZrO ₃	Ni/YSZ	4 mol% Ni doped SrZrO ₃
700	37.8	42.6	79.1	86.3
800	53.8	44.0	96.8	89.7
900	60.6	55.0	98.2	99.0

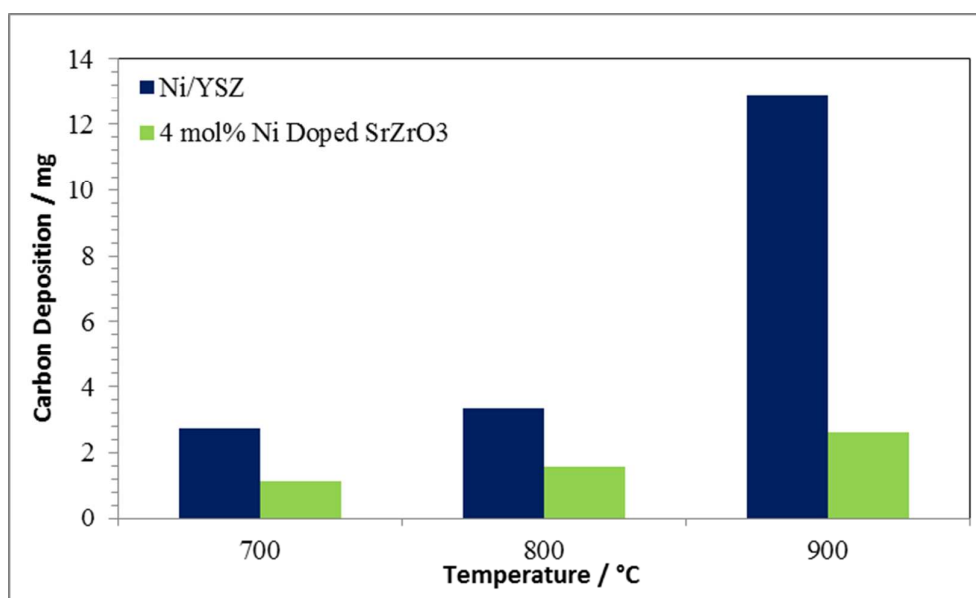


Figure 7: Comparison of solid carbon deposition at various temperatures for Ni/YSZ and 4 mol% Ni doped SrZrO₃

TPO analysis was performed after each reaction in order to quantify the carbon deposited. For Ni/YSZ going from 700 °C to 900 °C increased the deposited carbon by fivefold. This is due to the endothermic nature of the methane decomposition reaction which is the primary

carbon forming reaction above 800 °C. For 4 mol% Ni doped SrZrO₃ the increase in deposited carbon was not as dramatic, and this can be attributed to a lower tendency for the perovskite material to thermally decompose excess methane. Table 1 shows that Ni/YSZ decomposes more methane than 4 mol% Ni doped SrZrO₃ at all temperatures studied.

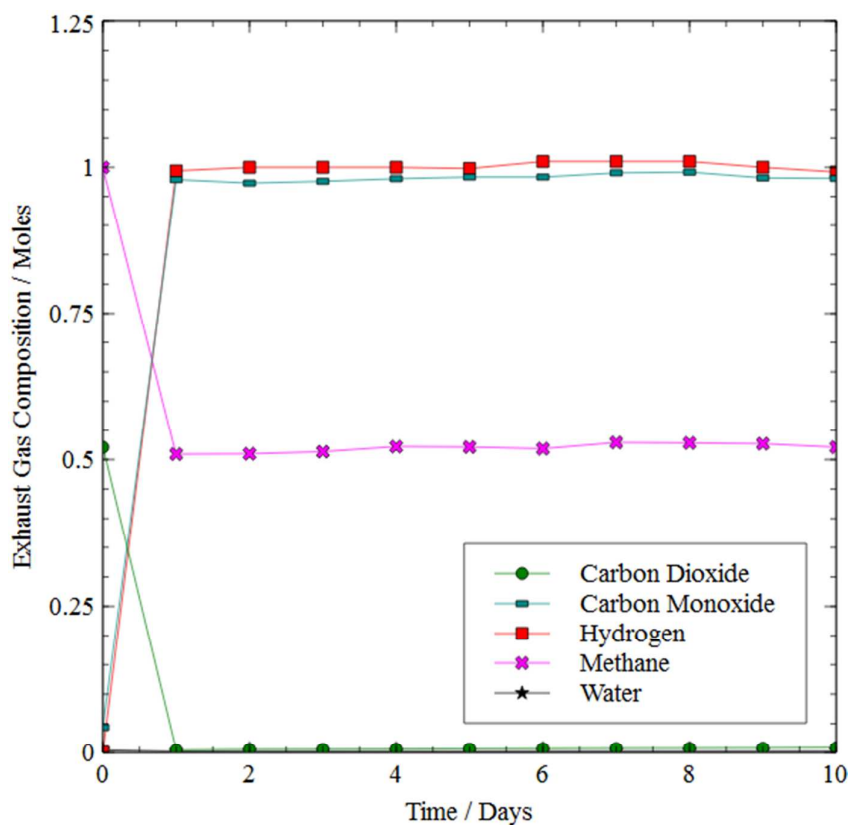


Figure 8: Biogas reformation at 850 °C for 240 hours over 4 mol% Ni doped SrZrO₃

In order to further evaluate the ability of 4 mol% Ni doped SrZrO₃ to resist formation of solid carbon, and also to ascertain the stability of this material for reforming biogas for extended periods of time, longer reactions were performed. These reactions were performed at 850 °C, as at 850 °C both the Boudouard reaction and methane pyrolysis are possible enabling the resistance to both types of carbon formation to be observed. Figure 8 shows that for 10 days a very stable reaction was observed with no observable loss of reforming activity. An H₂:CO

ratio of almost 1 is evident for the extent of the reaction showing that reforming, and not methane pyrolysis is the prevalent reaction pathway.

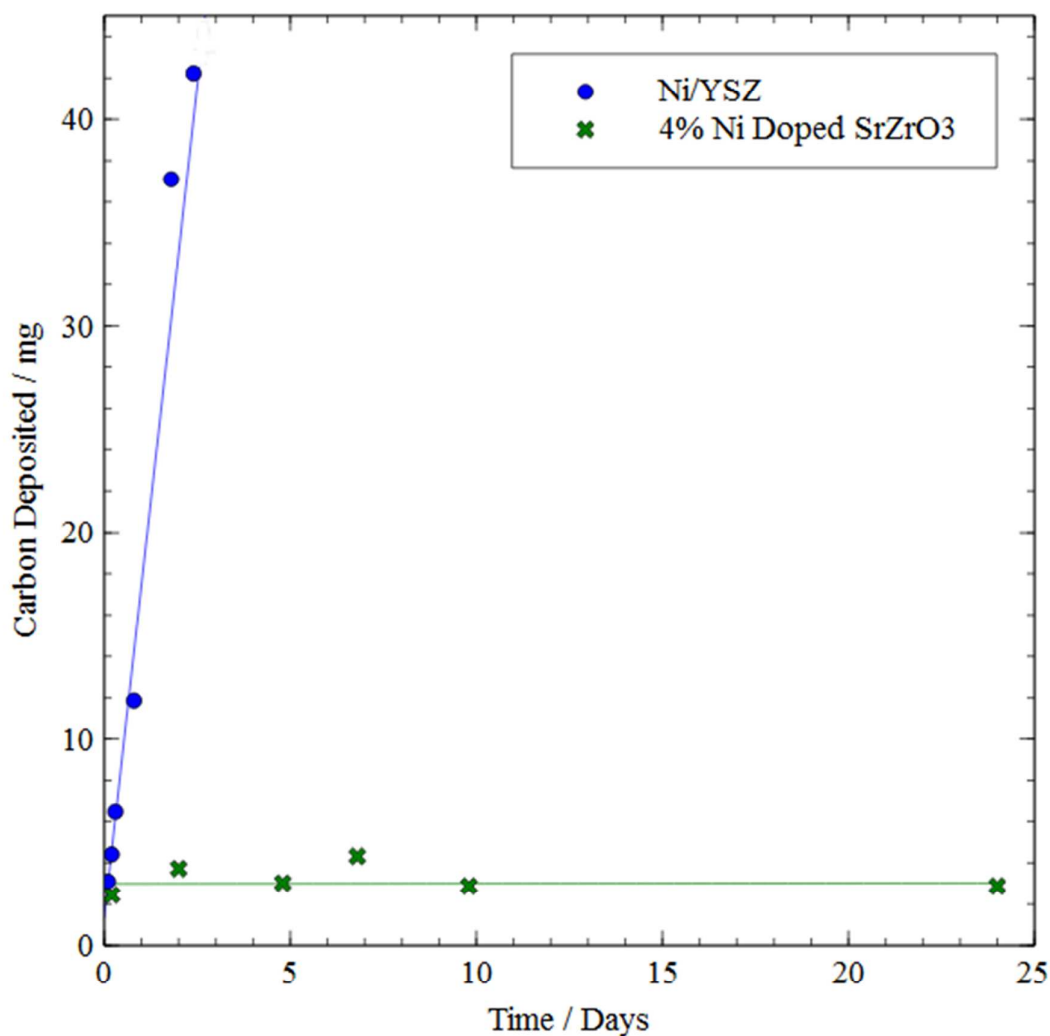


Figure 9: Comparison of solid carbon formation with time for Ni/YSZ and 4 mol% Ni doped SrZrO₃

Post-reaction TPO analysis (fig. 9) shows a linear relationship between reaction time for dry reforming methane at 850 °C over Ni/YSZ. This is expected as methane decomposition occurs for the extent of the reaction over Ni/YSZ. However this relationship is not seen when reforming methane under the same conditions with the 4 mol% Ni doped SrZrO₃ material. In the first few hours of reaction a comparable amount of carbon is deposited to

Ni/YSZ, this can be attributed to thermal decomposition of methane whilst the perovskite surface is pristine, after this no increase in deposited carbon can be seen for up to 240 hours, suggesting that either no methane decomposition is occurring or that a cycle of carbon deposition and carbon ‘cleaning’ is occurring on the surface. The significantly lower tendency to form carbon via the decomposition of excess methane in the reactant stream is due to the nickel actually being incorporated and effectively isolated within the perovskite structure, as opposed to existing as nickel particles supported on an oxide material.

5. Conclusions

A novel nickel-doped strontium zirconate perovskite (4 mol% Ni doped SrZrO₃) material has been synthesised using low temperature hydrothermal synthesis. The catalytic reforming activity of 4 mol% Ni doped SrZrO₃ was investigated for the dry reforming of simulated, methane-rich biogas. The material was found to be very efficient towards the conversion of methane-rich biogas at relatively low temperatures with high selectivity towards synthesis gas formation and extremely good resistance to carbon deposition. The material is at least as active as a conventional supported nickel catalyst with a significantly lower tendency to form carbon via the decomposition of excess methane in the reactant stream, this is due to the nickel being incorporated within the perovskite structure as opposed to being supported on an oxide material.

The 4 mol% Ni doped SrZrO₃ catalyst was found to have a very high selectivity towards the reforming reaction and little or no evidence of any undesirable side reactions occurring, most notably methane decomposition, shown by the H₂: CO ratio consistently being at the stoichiometric value predicted. This is also suggested to be due to nickel being isolated within the perovskite. 4 mol% Ni doped SrZrO₃ also displays evidence of being more active

at lower reaction temperatures than a standard Ni/YSZ anode material. The catalyst displays very low carbon deposition due to methane decomposition which does not increase over time, and as a result shows excellent stability.

The use of a catalyst produced by a green, low temperature hydrothermal route provides a potentially very attractive and sustainable source of useful chemicals from biogas that otherwise might be vented wastefully and detrimentally into the atmosphere.

Acknowledgements

The UK Engineering and Physical Sciences Research Council (EPSRC) is gratefully acknowledged for funding (Grant EP/I037059/1).

References

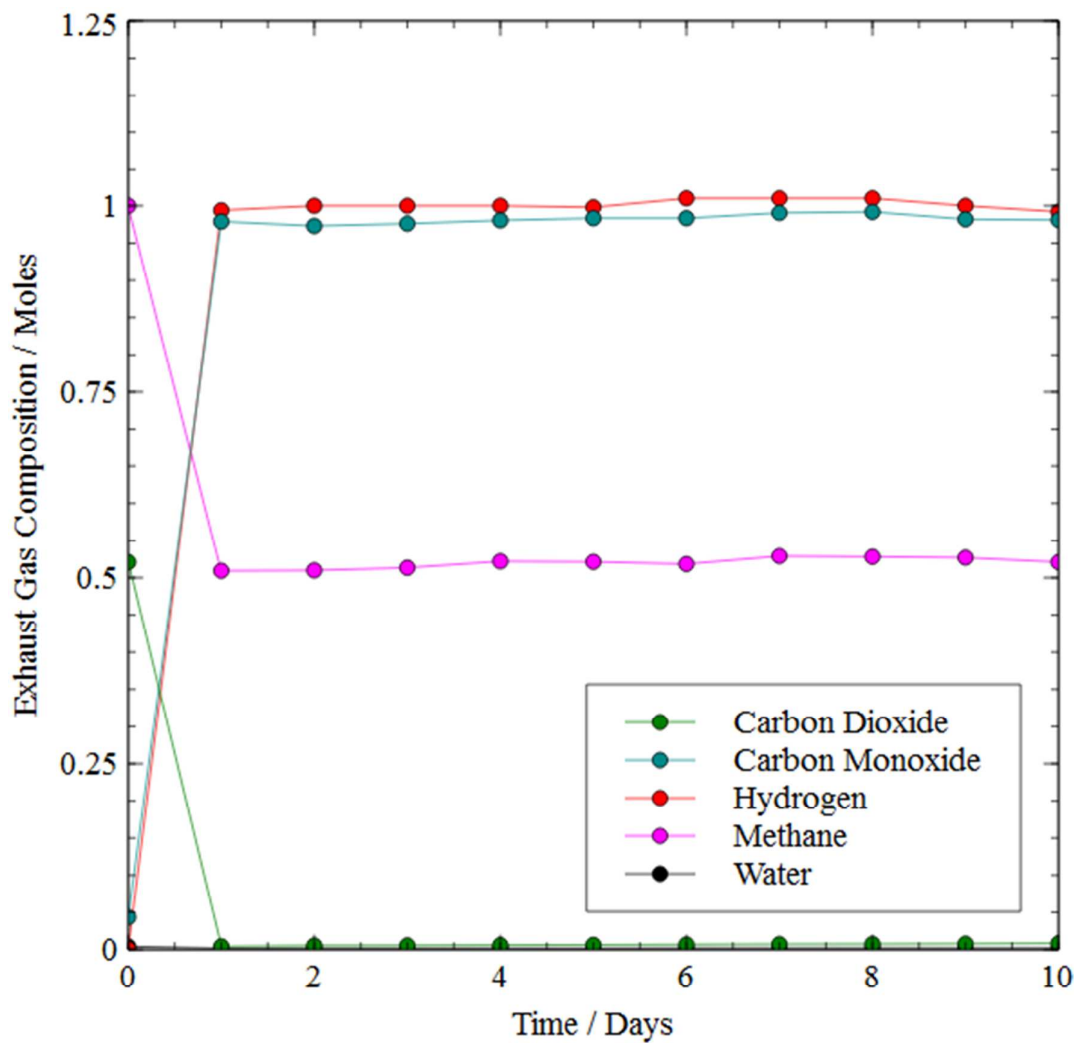
1. J. S. Kang, D. H. Kim, S. D. Lee, S. I. Hong, and D. J. Moon, *Appl. Catal. A Gen.*, 2007, **332**, 153–158.
2. C. Guerra, A. Lanzini, P. Leone, M. Santarelli, and N. P. Brandon, *J. Power Sources*, 2014, **245**, 154–163.
3. H. Arandiyan, J. Li, L. Ma, S. M. Hashemnejad, M. Z. Mirzaei, J. Chen, H. Chang, C. Liu, C. Wang, and L. Chen, *J. Ind. Eng. Chem.*, 2012, **18**, 2103–2114.
4. M. Santarelli, F. Quesito, V. Novaresio, C. Guerra, A. Lanzini, and D. Beretta, *J. Power Sources*, 2013, **242**, 405–414.
5. A. M. Robinson, M. E. Gin, and M. M. Yung, *Top. Catal.*, 2013, **56**, 1708–1715.
6. A. Serrano-Lotina and L. Daza, *J. Power Sources*, 2013, **238**, 81–86.
7. J. Singh and S. Gu, *Renew. Sustain. Energy Rev.*, 2010, **14**, 1367–1378.
8. Y. Li, S. Y. Park, and J. Zhu, *Renew. Sustain. Energy Rev.*, 2011, **15**, 821–826.
9. D. Deublein and A. Steinhauser, *Biogas from Waste and Renewable Resources An Introduction*, Wiley-VCH, Weinheim, 2008.
10. S. S. Kapdi, V. K. Vijay, S. K. Rajesh, and R. Prasad, *Renew. Energy*, 2005, **30**, 1195–1202.
11. Y. Shiratori, T. Ijichi, T. Oshima, and K. Sasaki, *Int. J. Hydrogen Energy*, 2010, **35**, 7905–7912.
12. I. Gavrielatos, V. Drakopoulos, and S. Neophytides, *J. Catal.*, 2008, **259**, 75–84.
13. W. Chen, G. Zhao, Q. Xue, L. Chen, and Y. Lu, *Appl. Catal. B Environ.*, 2013, **136-137**, 260–268.
14. S. Islam and J. M. Hill, *J. Power Sources*, 2011, **196**, 5091–5094.
15. A. Hornés, P. Bera, M. Fernández-García, A. Guerrero-Ruiz, and A. Martínez-Arias, *Appl. Catal. B Environ.*, 2012, **111-112**, 96–105.
16. K. Girona, J. Laurencin, J. Fouletier, and F. Lefebvre-Joud, *J. Power Sources*, 2012, **210**, 381–391.
17. I. P. Silverwood, N. G. Hamilton, A. R. McFarlane, J. Kapitán, L. Hecht, E. L. Norris, R. M. Ormerod, C. D. Frost, S. F. Parker, and D. Lennon, *Phys. Chem. Chem. Phys.*, 2012, **14**, 15214–15225.

18. H. Sumi, Y. Lee, H. Muroyama, T. Matsui, M. Kamijo, S. Mimuro, M. Yamanaka, Y. Nakajima, and K. Eguchi, *J. Power Sources*, 2011, **196**, 4451–4457.
19. R. J. Gorte and J. M. Vohs, *J. Catal.*, 2003, **216**, 477–486.
20. N. E. Kiratzis, P. Connor, and J. T. S. Irvine, *J. Electroceramics*, 2009, **24**, 270–287.
21. H. He and J. M. Hill, *Appl. Catal. A Gen.*, 2007, **317**, 284–292.
22. M. Kawano, H. Yoshida, D. Ueno, S. Hashigami, and T. Inagaki, *Electrochem. Soc. Trans.*, 2012, **42**, 305–311.
23. J. Jia, E. Tanabe, P. Wang, K. Ito, H. Morioka, Y. Wang, and T. Shishido, *Catal. Letters*, 2001, **76**, 183–192.
24. T. Hayakawa, S. Suzuki, J. Nakamura, T. Uchijima, and S. Hamakawa, *Appl. Catal. A Gen.*, 1999, **183**.
25. A. Serrano-Lotina, L. Rodríguez, G. Muñoz, and L. Daza, *J. Power Sources*, 2011, **196**, 4404–4410.
26. A. Sauvet, *Solid State Ionics*, 2004, **167**, 1–8.
27. H. Takahashi, T. Takeguchi, N. Yamamoto, M. Matsuda, E. Kobayashi, and W. Ueda, *J. Mol. Catal. A Chem.*, 2011, **350**, 69–74.
28. J. Z. Staniforth and R. M. Ormerod, *Catal. Letters*, 2002, **81**, 19–23.
29. J. Z. Staniforth and K. Kendall, *J. Power Sources*, 2000, **86**, 401–403.
30. S. Mcintosh and R. J. Gorte, *Chem. Rev.*, 2004, **104**, 4845–4865.
31. M. Lo Faro, V. Antonucci, P. L. Antonucci, and A. S. Arico, *Fuel*, 2012, **102**, 554–559.
32. Z. Jiao, N. Shikazono, and N. Kasagi, *J. Power Sources*, 2011, **196**, 8366–8376.
33. A. Lanzini and P. Leone, *Int. J. Hydrogen Energy*, 2010, **35**, 2463–2476.
34. G. J. Offer, J. Mermelstein, E. Brightman, and N. P. Brandon, *J. Am. Ceram. Soc.*, 2009, **92**, 763–780.
35. EG&G Technical Services, *Fuel Cell Handbook*, U.S. Department of Energy, Morgantown, West Virginia, Seventh Ed., 2004.
36. A. W. F. Libby, S. Url, and S. Levine, *Science* 2013, **171**, 499–500.
37. K. Takehira, *J. Catal.*, 2002, **207**, 307–316.

38. M.-C. Zhan, W.-D. Wang, T.-F. Tian, and C.-S. Chen, *Energy and Fuels*, 2010, **24**, 764–771.
39. C. S. Lau, A. Tsolakis, and M. L. Wyszynski, *Int. J. Hydrogen Energy*, 2010, **36**, 397–404.
40. J. Sfeir, *J. Catal.*, 2001, **202**, 229–244.
41. A. S. B. Ruyan and G. Rustum, *Mater. Res. Innov.*, 2000, **4**, 3–26.
42. M. Niederberger, N. Pinna, J. Polleux, and M. Antonietti, *Angew. Chem. Int. Ed. Engl.*, 2004, **43**, 2270–2273.
43. W. Zheng, W. Pang, and G. Meng, *Solid State Ionics*, 1998, **108**, 37–41.
44. R. J. Darton, S. S. Turner, J. Sloan, M. R. Lees, and R. I. Walton, *Cryst. Growth Des.*, 2010, **10**, 3819–3823.
45. D. R. Modeshia, R. J. Darton, S. E. Ashbrook, and R. I. Walton, *Chem. Commun.*, 2009, **3430**, 68–70.
46. H.-C. Yu, K.-Z. Fung, T.-C. Guo, and W.-L. Chang, *Electrochim. Acta*, 2004, **50**, 811–816.
47. Z. Shao, W. Zhou, and Z. Zhu, *Prog. Mater. Sci.*, 2012, **57**, 804–874.
48. B. L. Cushing, V. L. Kolesnichenko, and C. J. O'Connor, *Chem. Rev.*, 2004, **104**, 3893–3946.
49. S.E Evans, O. J. Good, J.Z. Staniforth, R.M. Ormerod, and R.J. Darton, *RSC Advances*, 2014, **4**, 30816-30819.
50. J.Z. Staniforth, S.E. Evans, R.J. Darton and R.M. Ormerod, *Dalton Trans.*, 2014, DOI10.1039/C4DT01288G
51. C. J. Laycock, J. Z. Staniforth, and R. M. Ormerod, *Electrochem. Soc. Trans.*, 2009, **16**, 177–188.
52. A. M. Beale, M. Paul, G. Sankar, R. J. Oldman, C. R. A. Catlow, S. French, and M. Fowles, *J. Mater. Chem.*, 2009, **19**, 4391.
53. S. Tomiyama, R. Takahashi, S. Sato, T. Sodesawa, and S. Yoshida, *Appl. Catal. A Gen.*, 2003, **241**, 349–361.
54. G. Valderrama, C. Urbina de Navarro, and M. R. Goldwasser, *J. Power Sources*, 2013, **234**, 31–37.

A nickel doped perovskite catalyst for reforming methane rich biogas with minimal carbon deposition

Samuel E. Evans*, John Z. Staniforth, Richard J. Darton, R. Mark Ormerod*



In this paper we describe the use of a perovskite material synthesised by a low temperature route for the conversion of methane-rich biogas into synthesis gas, which shows high activity and selectivity and extremely good resistance to deleterious carbon deposition.